02

Modeling Raman spectra of glycine and alanine within a discrete-continuum water environment and with considering anharmonic effects

© A.V. Golovin[1], I.V. Krauklis[1,¶], A.A. Nazarova[1], Yu.V. Chizhov[1], A.V. Shurukhina[2]

[1] St. Petersburg State University, St. Petersburg, Russia
[2] Saint-Petersburg State University, Laboratory of „Crystal photonics“, Saint-Petersburg, Russia

e-mail: i.krauklis@spbu.ru

Received July 19, 2025
Revised October 07, 2025
Accepted December 21, 2025

Raman spectra of glycine and alanine in crystalline form and in buffered solution were obtained. It was demonstrated that accounting for the influence of the water environment within discrete-continuum models Gly(ZW)+7H_2O and Ala(ZW)+7H_2O allows for good agreement between experimental and theoretical data in the harmonic approximation. Anharmonic calculations of zwitterions Gly(ZW) and Ala(ZW) were performed using the generalized vibrational perturbation theory of second order (GVPT2) at the B3LYP(+GD3)/def2TZVPP and MP2(FC)/def2TZVPP levels of theory. Relative anharmonic frequency shifts of these zwitterions were analyzed, taking into account Fermi and Darling-Dennison resonances. It was shown that the GVPT2 method provides acceptable agreement with experimental Raman spectra of glycine and alanine if several low-frequency modes are excluded during the VPT2 calculation to eliminate non-physical results.

Keywords: α-amino acids, zwitterionic state, generalized vibrational perturbation theory of second order (GVPT2), anharmonic and harmonic frequencies, Fermi and Darling-Dennison resonances, density functional theory, discrete-continuum water model, Raman spectra.

DOI: 10.61011/EOS.2026.01.63218.8413-25

Introduction

The physico-chemical characteristics and spectral properties of α-amino acids in an aqueous medium and crystalline state are determined by the zwitterionic structure with spatially separated charges $NH_3^+-CHR-COO^-$, where R — lateral radical. The simplest αamino acids, such as glycine Gly,(R=−H) and alanine Ala,(R=$-CH_3$), have been well studied by various theoretical and experimental methods [1–3], which makes them convenient model structures. Apart from the X-ray diffraction analysis, vibrational spectroscopy remains a powerful tool for studying amino acids, short peptides, and secondary protein structures, since this method is highly sensitive to structural changes and interactions in hydrated media [4,5].

In quantum chemical modeling of zwitterions of α-amino acids, it is necessary to allow for the environmental impact as a stabilizing factor due to the presence of dipole-dipole intermolecular interactions and the formation of additional hydrogen bonds. Currently, it is customary to use discrete-continuous solvation shell models with a variable number of water molecules to account for solvation effects [6–9]. The discrete model, as a rule, represents the first coordination sphere of water molecules around a zwitterion, and long-acting solvation effects are taken into account using the polarizable continuum model (PCM). The question of the number of water molecules needed to stabilize a specific zwitterion and their relative positions is being debated in the scientific community [10–12]. In the future, such model systems can be used to interpret various vibrational spectra of αamino acids. For example, there are known studies of [6,7], in which using B3LYP/6-31++G* method a vibration analysis of the molecular complexes of Gly+12H_2O and Ala+5H_2O was performed for comparison with experimental infrared (IR) and Raman spectra (RS) of glycine and alanine.

In this paper, the RS spectra of glycine and alanine in buffer solution and in the crystalline state are presented. To describe the RS spectra of glycine and alanine in buffer solution within the framework of the harmonic approximation we used the proposed in [13] discrete-continuum models of zwitterions+7H_2O and Ala(ZW)+7H_2O, containing seven water molecules which saturate all hydrogen couplings of the functional groups $-NH_3^+$ and $-COO^-$. In this case, one water molecule acts as a bridge between these groups (Fig. 1, *a, b*).

For a more accurate interpretation of the biomolecule spectra, it is desirable to take into account the anharmonicity of vibrations [14]. Despite the availability of anharmonic calculations in modern quantum chemical programs, their use for the theoretical estimation of vibrational frequencies of α-amino acids is quite rare [15]. The zwitterions of α-amino acids are polyatomic structures with a large number of vibrational modes, between which Fermi res-

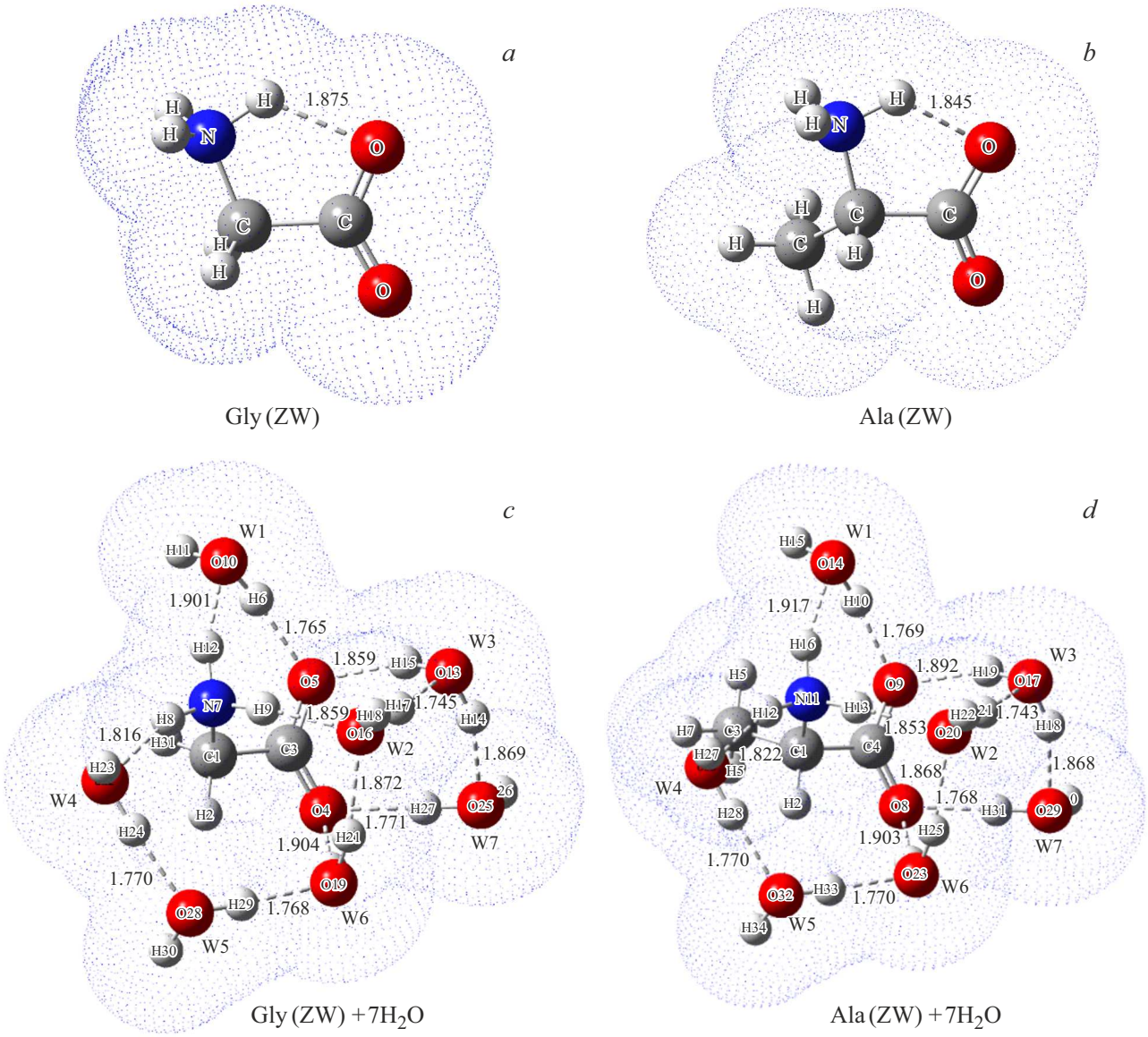

Figure 1. Discrete-continuum models of glycine and alanine zwitterions.

onances [16] and Darling-Dennison resonances [17] may occur, which complicates the analysis and interpretation of the spectra. In the second part of the article, we analyze the anharmonic frequencies of glycine and alanine zwitterions obtained using the generalized second-order vibrational perturbation theory (GVPT2) [18]. Using methods B3LYP(+GD3)/def2TZVPP and MP2(FC)/def2TZVPP the harmonic and inharmonic frequencies were analyzed for Gly(ZW) and Ala(ZW) zwitterions within a PCM-model of the aqueous solvent (Fig. 1, *c, d*). This simple model can be extremely useful for characterizing the bands of Raman spectra of amino acids both in an aqueous medium and in a crystal, since the crystal field has little effect on the intramolecular bonds of functional groups $-NH_3^+$ and $-COO^-$ [19,20].

Research methods

Experiment

Experimental RS spectra of glycine and alanine were obtained using Horiba Jobin-Yvon LabRam HR800 spectrometer with Olympus BX41 microscope at room temperature. A semiconductor solid-state laser with a wavelength of 532 nm and a sample power of 10 MW was used. Diffraction grating had 1800 lines/mm. The confocal opening was 100 μ. The solid phases of amino acids were studied using a 50x lens, and buffer solutions (Gly, Ala) using a 10x lens. Optical resolution was 2 cm^{-1}. The experiment was carried out in the Resource Center „Geomodel“ SPbGU [21].

Sodium hydrophosphate (pH 6.86) was used to prepare the buffer solution. The molar concentrations of amino

acids in buffer solutions were taken as follows: C (Gly, Ala) = 1.0 M/L. The spectrum of the buffer itself was subtracted from the spectra of amino acids obtained in the buffer solution. All spectra were processed by MagicPlot [22].

Theory

Quantum chemical analysis of the structures geometry was carried out at the level of density functional theory B3LYP(+GD3)/def2TZVPP and perturbation theory MP2(FC)/def2TZVPP using Gaussian package 16 [23], installed on a high-performance Huawei cluster in Computational Center SPbGU [24]. The calculations included Grimme's dispersion correction GD3 to account for weak intermolecular interactions. The geometry of conformers was optimized using the enhanced VeryLight convergence criterion and Grid=UltraFine grid for numerical integration, recommended for DFT calculations of molecules with a large number of soft modes (groups $-CH_3$, $-NH_3$). A criterion for reaching the local minimum was the absence of imaginary frequencies of normal vibrations.

For the discrete-continuum models of Gly(ZW)+7H_2O and Ala(ZW)+7H_2O the vibration analysis only using method B3LYP+GD3/def2TZVPP in harmonic approximation. The types of vibrations were determined in Veda [25] program, using potential energy distribution analysis (PED), as well as by visualizing them in GaussView 6.0 program.

The second-order generalized vibrational perturbation theory (GVPT2) [18], implemented in Gaussian 16, was used to calculate the anharmonic frequencies of Gly(ZW) and Ala(ZW) zwitterions. GVPT2 method is an extension of the standard VPT2 theory, specifically designed to better account for the Fermi and Darling-Dennison resonances. It uses a hybrid approach that involves identification and removal of resonant modes from VPT2 equations, and then their variational processing, which allows us to obtain new mixed frequencies and wave functions for resonant modes. This provides a more accurate description of the oscillatory frequencies and intensities. Using DataMod key=SkipPT2=Modes „deactivation" of some low-frequency vibrational modes was performed during VPT2 calculation to correct improbable results.

Results and discussion

Experiment

Experimental RS spectra of crystalline powders of glycine and alanine, as well as their buffer solutions, are shown in Fig. 2 in the range 300−3400 cm^{-1}. The intensity scale for powders is on the right, for buffer solutions — on the left. In general, there is a good correlation of the main bands of both glycine and alanine. In Table 1 and 2 experimental bands are compared with the calculated harmonic and anharmonic frequencies of Gly(ZW) and Ala(ZW) zwitterions, and in Table 3 — with harmonic frequencies for discrete-continuum models of Gly(ZW)+7H_2O and Ala(ZW)+7H_2O. The interpretation of the experimental RS spectra of glycine and alanine based on the calculations is presented below.

Interpretation of RS spectra of glycine in the harmonic approximation

Region above 3000 cm^{-1} As found from the analysis of Gly(ZW) zwitterion(Table. 1), the most intense band in powder and buffer solution at 2973 cm^{-1} correlates with symmetric stretching of the hydrophobic CH_2-group $\nu_{sym}(C_\alpha H_2)$. Valence stretching of ν(N−H) coupling also lies in this range which is because of its additional hydrogen binding with $-COO^-$ group. The second intensive band at 3007 cm^{-1} (in the buffer — 3014 cm^{-1}) is related to the valence antisymmetric vibration $\nu_{asym}(C_\alpha H_2)$. Medium-intensity wide band in powder at 3145 cm^{-1} (in buffer — arm of 3148 cm^{-1}) is related to the symmetric $\nu_{sym}(NH_2)$ and asymmetric $\nu_{asym}(NH_2)$ stretching of $-NH_3^+$ group, which in the buffer solution are quenched by interactions with water molecules. Harmonic frequency scaling for the model Gly(ZW)+7H_2O (table. 3) gives a good agreement with the experimental data for the buffer solution, which is clearly shown in Fig. 3, *a*. In the region of 3400 cm^{-1}, a low-intensity wide band is observed, which is formed by collective stretching of O−H couplings of water molecules.

Region 1500−1700 cm^{-1} In this region of RS spectrum of Gly powder, low-intensity bands are observed at 1517, 1570, 1633, and 1670 cm^{-1}, resulting from angular bends of δ(HNH) group $-NH_3^+$ and antisymmetric stretching of $\nu_{asym}(CO_2)$. Additionally, the analyzed molecular complex Gly(ZW)+7H_2O shows that the angular bends of NH_3^+ group are largely combined with the deformational angular modes $\delta(H_2O)$ of the surrounding water molecules resulting in a severe blurring of these bands in 1626 cm^{-1} region in the buffer.

Region 1200−1500 cm^{-1} Several intense bands are observed in this region of RS spectrum of glycine both in powder and in buffer solution. The appearance of these bands is mainly due to the deformational vibrations of R= −H lateral radical. The most intensive band at 1325 cm^{-1} (in buffer — 1330 cm^{-1}) is caused by angular vibration $\delta(C_\alpha H_2)$ where torsional twisting of $\tau(HC_\alpha CO)$ is also added. The symmetrical stretching of the carboxyl group $\nu_{sym}(CO_2)$ and stretching of $\nu(C_\alpha - C)$ also fall into this band. The intense band at 1413 cm^{-1} (in buffer — 1415 cm^{-1}) corresponds to a symmetrical angular bend $\delta_{sym}(NH_3)$, which is in good agreement with the same frequency of alanine. These bands can be considered reference for glycine. The intense band at 1455 cm^{-1} (in buffer — 1446 cm^{-1}) is associated with torsional

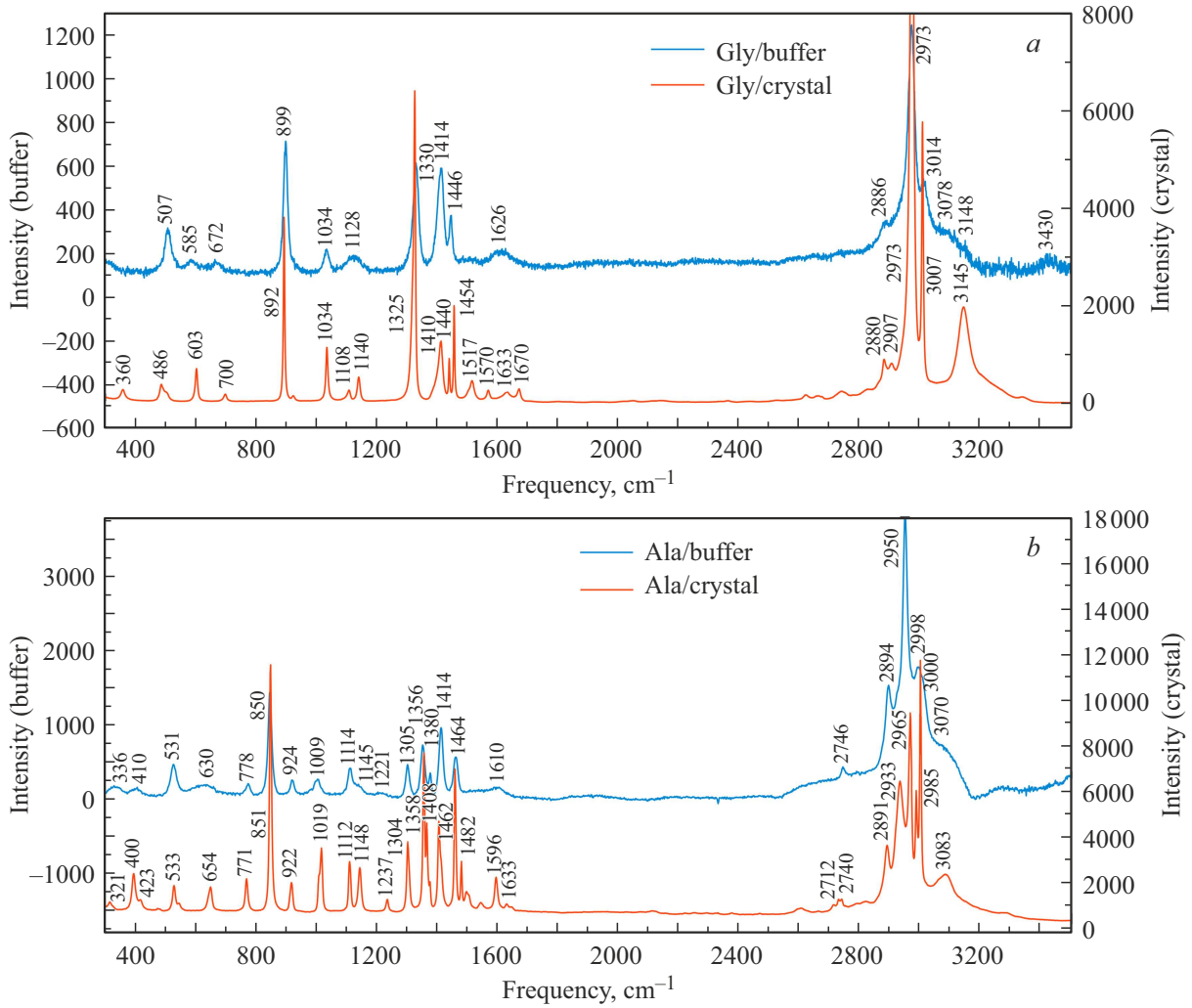

Figure 2. RS spectra of glycine (a) and alanine (b) as a crystalline powder and in buffer solutions within 300 – 3500 cm^{-1}.

twisting $\tau(HC_\alpha CO)$, added with deformational angular vibration $\delta(C_\alpha H_2)$.

Region below 1200 cm^{-1} Low-intensity bands at 1108 and 1140 cm^{-1} are associated with deformation torsional twisting $\tau(HNC_\alpha C)$ and $\tau(NC_\alpha CO)$, added with angular bends $\delta(HNH)$. The mid-intensity band at 1034 cm^{-1} corresponds to the stretching of $\nu(N-C_\alpha)$ coupling, it retains its position and intensity in the buffer solution, therefore it can be attributed to the reference ones. In said region the most intensive band is the one at 892 cm^{-1} (899 cm^{-1} in the buffer) corresponding to the stretching of $\nu(C_\alpha-C)$ coupling with some additional angular vibration $\delta(C_\alpha CO)$. This band can also be considered a reference band for glycine. The mid-intensity band in the powder at 603 cm^{-1} correlates with the deformation torsional vibrations of $\tau(HC_\alpha CO)$ and $\tau(NC_\alpha CO)$, which are partially quenched in the buffer solution due to interactions with surrounding water molecules, as evidenced by the blurring of 585 cm^{-1} band in the spectrum of the buffer solution. The low-intensity band at 486 cm^{-1} (in buffer — 507 cm^{-1}) is mainly associated with deformation bending $\delta(C_\alpha CO)$ with some added stretching of $\nu(C_\alpha-C)$ couplings. A weak intensity band is observed in glycine powder at 360 cm^{-1}, which correlates with the angular vibration of the molecular skeleton $\delta(C_\alpha CO)$.

Interpretation of RS spectra of alanine in the harmonic approximation

Region above 3000 cm^{-1} A series of intense vibrations in this region of RS spectrum is associated with various combinations of stretching of groups -$C_\beta H_3$, –NH_3 and –$C_\alpha H$ (Table 2). Groups –$C_\beta H_3$ and –$C_\alpha H$ are hydrophobic, so their vibrations are more active. The mid-intensity band at 2891 cm^{-1}(in buffer — 2894 cm^{-1}) correlates with symmetrical stretching of group $\nu_{sym}(C_\beta H_3)$. Intensive bands at 2933 and 2965 cm^{-1} (in the buffer — band at 2950 cm^{-1} with an arm of 2925 cm^{-1}) are related to combinations of stretching of $\nu(C_\alpha-H)$ and asymmetric stretching of $\nu_{asym}(C_\beta-H_2)$. The intense band at 2985 cm^{-1} (in the

Table 1. Experimental RS bands (cm^{-1}) of glycine and calculated harmonic and anharmonic frequencies (cm^{-1}) of Gly(ZW) zwitterion, their absolute ($\Delta\nu = \nu^{harm} - \nu^{anh}$) and relative $\left(\frac{|\Delta\nu|}{\nu^{harm}} \cdot 100\%\right)$ shifts obtained by B3LYP(+GD3) and MP2(FC) methods.

Experiment		B3LYP+GD3/def2TZVPP				B3LYP/def2TZVPP				MP2(FC)/def2TZVPP				Number and type of vibrations, PED %
crystal	buffer	ν^{harm}	ν^{anh}	$\Delta\nu$	$\frac{\lvert\Delta\nu\rvert}{\nu^{harm}}$	ν^{harm}	ν^{anh}	$\Delta\nu$	$\frac{\lvert\Delta\nu\rvert}{\nu^{harm}}$	ν^{harm}	ν^{anh}	$\Delta\nu$	$\frac{\lvert\Delta\nu\rvert}{\nu^{harm}}$	
3145(m)	3148(sh)	3552	3355	−198	5.6	3552	3334	−218	6.1	3607	3292	−315	8.7	(24)$\nu_{asym}(NH_2)$ 100
		3497	3315	−183	5.2	3498	3297	−201	5.7	3538	3224	−314	8.9	(23)$\nu_{sym}(NH_2)$ 99
3007(s)	3014(s)	3170	2972	−199	6.3	3171	3013	−157	5.0	3234	3077	−157	4.9	(22)$\nu_{asym}(C_\alpha H_2)$ -100
		3158	2886	−272	8.6	3146	2805	−341	**10.8**	3167	3042	−126	4.0	(21)ν(N−H) 94
2973(s)	2973(s)	3112	2944	−168	5.4	3113	2987	−126	4.0	3143	2737	−406	**12.9**	(20)$\nu_{sym}(C_\alpha H_2)$ 97
1670(w)		1663	1611	−52	3.1	1664	1617	−47	2.8	1687	1659	−28	1.7	(19) δ(HNH) 41, ν_{asym} (CO_2) -35
1630(w)	1626(w)	1655	1751	95	5.7	1656	1630	−25	1.5	1669	1626	−43	2.6	(18) δ(HNH) 75
1570(w)		1639	1461	-178	**10.9**	1640	1462	−178	**10.9**	1650	1394	−256	**15.5**	(17) δ(HNH) 38, ν_{asym} (CO_2) 46
1455(m)		1474	1364	−110	7.5	1475	1435	−40	2.7	1486	1325	−160	**10.8**	(16) τ($HC_\alpha CO$) 52, $\delta_{sym}(HC_\alpha H)$ 36
1440(m)	1446(m)	1447	1446	−1	0.07	1446	1355	−91	6.3	1432	1449	17	1.2	(15) $\delta_{sym}(NH_3)$ 79, $\delta_{sym}(HC_\alpha H)$ 10
1413(m)	1415(m)	1372	1336	−36	2.6	1373	1318	−55	4.0	1389	1351	−38	2.7	(14) $\nu_{sym}(CO_2)$, $\nu(C_\alpha - C)$ 67
1325(s)	1330(s)	1330	1118	−211	**15.9**	1332	1266	−66	5.0	1331	1235	−96	7.2	(13) $\delta_{sym}(HC_\alpha H)$ 42, τ($HC_\alpha CO$) -28
		1306	1193	−113	**8.7**	1309	1259	−49	3.7	1321	1235	−86	6.5	(12) δ(HCN) 67
1140(w)	1128(w)	1111	919	−191	**17.2**	1112	962	−150	13.5	1117	874	−243	**21.8**	(11) τ($HNC_\alpha C$) -68, δ(HNH) 10
1108(w)		1099	1017	−82	7.5	1103	1043	−60	5.4	1108	1098	−10	0.9	(10) τ($HNC_\alpha C$) 60, δ(HNH) 15
1034 (m)	1034(m)	990	893	−96	**9.7**	993	898	−95	**9.6**	1041	892	−149	**14.3**	(9) ν(N-C_α) 77
925(w)		940	859	−81	**8.6**	940	817	−123	**13.1**	945	744	−202	**21.4**	(8) τ($HNC_\alpha C$) 62, δ(HCN) -11
892 (s)	898(s)	864	851	−13	1.5	867	843	−24	2.8	880	869	−11	1.3	(7) $\nu(C_\alpha - C)$ 52, $\delta(C_\alpha CO)$ 18
700(w)	672 (w)	673	680	7	1.0	676	666	−10	1.5	686	684	−2	0.3	(6) $\delta(C_\alpha CO)$ 66, V(C_α-C) -16
603(m)	585(w)	575	462	−112	**19.5**	577	575	−2	0.3	575	566	−8	1.4	(5) τ($HC_\alpha CO$) 54, τ($HNC_\alpha C$) 18
486(w)	507(w)	497	473	−24	4.8	500	492	−8	1.6	509	502	−7	1.4	(4) $\delta(C_\alpha CO)$ 63, $\nu(C_\alpha - C)$ -18
360(w)		290	390	100	**34.5**	298	228	−71	**23.8**	307	293	−14	4.6	(3) $\delta(C_\alpha CO)$ 86
		258	497	238	**92.2**	269	29	−241	**90**	265	−58	−324	**122**	(2) τ($HNC_\alpha C$) 79
		106	−375	−481	**454**	110	−468	−578	**526**	111	−957	−1068	**962**	(1) τ($HNC_\alpha C$) 63, τ($HNC_\alpha C$) -15

Designations: ν — valence stretching, δ — deformation scissor vibration (bending), τ — deformation torsional vibration (torsion), ω(ABCD) — a kind of torsional vibration, denotes the angle between AD vector and BCD plane, sym and asym — symmetric and asymmetric vibrations.

buffer — wide band at 2998 cm^{-1}) is associated with the stretching of $\nu(C_\beta - H)$. The band 3000 cm^{-1} falls into the same region, which corresponds, according to calculations, to the stretching ν(N−H). The low-intensity wide band at 3083 cm^{-1} correlates with symmetric $\nu_{sym}(NH_2)$ and asymmetric $\nu_{asym}(NH_2)$ vibrations of -NH_3 group.

Region above 1500-1700 cm^{-1} In this region of RS spectrum of alanine, low-intensity bands are observed, which occur mainly due to angular bends of the –NH_3 group and asymmetric valence stretching of $\nu_{asym}(CO_2)$. The band of medium intensity at 1596 cm^{-1} in powder corresponds to an asymmetric stretching $\nu_{asym}(CO_2)$ and a symmetrical scissor vibration $\delta_{sym}(NH_3)$. Low-intensity bands at 1548, 1633, and 1648 cm^{-1} are associated with asymmetric scissor vibrations of $\delta_{asym}(NH_2)$ and asymmetric stretching of $\nu_{asym}(CO_2)$, to which deformation scissor vibrations of H_2O molecules are added in the buffer (Table 3). One wide band is observed in the buffer solution at 1630 cm^{-1}, since the deformation angular vibrations of group —NH_3 are largely quenched by the angular modes of the surrounding water molecules. Harmonic frequency scaling for model Ala(ZW) + $7H_2O$ provides a very good agreement with the experimental spectrum of alanine in buffer solution (Fig. 3, *b*).

Region 1300−1500 cm^{-1} In this region, several intense bands are observed in the Raman spectra of alanine associated with stretching of group ν_2 (CO_2), as well as with deformation vibrations of the lateral radical $-C_\beta H3$ and group $-C_\alpha H$. As seen from calculations (Table 2), intensive band at 1462 cm^{-1} (in the buffer — 1464 cm^{-1}) and mid-intensity band at 1482 cm^{-1} correlate with the combinations of angular bends $\delta(HC_\beta H)$ and torsional vibrations $\tau(HC_\beta C_\alpha N)$. Intense band at 1408 cm^{-1} (in buffer — 1414 cm^{-1}) and arm at 1378 cm^{-1} (in the buffer — 1380 cm^{-1}) are associated with a combination of symmetrical scissor vibrations of the groups $\delta_{sym}(CH_3)$ and δ_{sym}(NH). The mid-intense band at 1367 cm^{-1} is related to the torsional vibration $\tau(HC_\alpha CO)$ which is complemented with an angular vibration $\delta(HC_\alpha C_\beta)$. The intensive band at 1358 cm^{-1} (in the buffer — 1356 cm^{-1}) corresponds to the combination of valence stretching $\nu_{sym}(CO_2)$ and $\nu(C_\alpha - CO_2)$. This is one of the alanine

Table 2. Experimental RS bands (cm^{-1}) of alanine and designed harmonic and inharmonic frequencies (cm^{-1}) of Ala(ZW) zwitterion, their absolute ($\Delta = \nu^{harm} - \nu^{anh}$) and relative $\left(\frac{|\Delta\nu|}{\nu^{harm}} \cdot 100\%\right)$ shifts obtained by B3LYP(+GD3) and MP2(FC) methods.

Experiment		B3LY+GD3/def2TZVPP				B3LYP/def2TZVPP				MP2(FC)/def2TZVPP				Number and type of vibrations,
crystal	buffer ν^{harm}	ν^{anh}	$\delta\nu$	$\frac{\|\Delta\nu\|}{\nu^{harm}}$	ν^{harm}	ν^{anh}	$\Delta\nu$	$\frac{\|\Delta\nu\|}{\nu^{harm}}$	ν^{harm}	ν^{anh}	$\Delta\nu$	$\frac{\|\Delta\nu\|}{\nu^{harm}}$	PED %	
3083 (m)	3070 (sh)	3544	3417	−127	3.6	3545	3361	−184	5.2	3594	3401	−193	5.4	(1) $\nu_{asym}(NH_2)$ 98
		3486	3292	−194	5.6	3487	3315	−172	4.9	3523	3312	−211	6.0	(2) $\nu_{sym}(NH_)$ 97
3000 (s)	2998(s)	3159	2648	−511	**16.2**	3139	2960	−179	5.7	3201	3102	−99	3.1	(3) ν(N−H) 96
2985 (s)		3139	3033	−106	3.4	3136	2633	−503	**16.0**	3180	3071	−109	3.4	(4) $\nu(C_\alpha-H)$85
2965(s)	2950(s)	3109	2977	−132	4.3	3109	3024	−85	2.7	3165	3043	−122	3.9	(5) $\nu(C_\alpha-H)-\nu_{asym}(C_\beta H_2)$ 99
2933(s)	2925(sh)	3091	2990	−101	3.3	3092	2981	−110	3.6	3130	2645	−485	**15.5**	(6) $\nu(C_\alpha-H)-\nu(C_\alpha-H)$ -95
2891(m)	2894(s)	3039	2908	−131	4.3	3041	2899	−142	4.7	3085	2983	−102	3.3	(7) $\nu_{sym}(C_\beta H_3)$ 84
1633(w)	1610(w)	1660	1799	139	**8.4**	1659	1533	−126	7.6	1681	1646	−35	2.1	(8) δ(HNH) 61, τ(HNC$_\alpha$C$_\beta$)21
1596(m)		1648	1578	−70	4.3	1649	1598	−51	3.1	1664	1722	58	3.5	(9) $\nu_{as}(CO_2)$ −53, δ(HNH) 26
1550(w)		1622	1727	105	6.5	1623	1843	220	**13.6**	1633	1445	−188	**11.5**	(10) δ(HNH) 51, $\nu_{as}(CO_2)$ 20
1482(m)		1489	1633	144	**9.7**	1488	1543	55	3.7	1503	1486	−17	1.1	(11) δ(HCH)76, τ(HC$_\beta$C$_\alpha$N) 20
1462(s)	1464(s)	1484	1499	15	1.0	1484	1487	3	0.2	1501	1451	−50	3.3	(12) δ(HCH)73, τ(HC$_\beta$C$_\alpha$N) 22
1408(m)	1414(m)	1434	1275	−159	**11.1**	1434	1421	−13	0.9	1432	1374	−58	4.1	(13) $\delta_{sym}(NH_3)$ 61, $\delta_{sym}(CH_3)$12
1378(sh)	1380(w)	1411	1400	−11	0.8	1411	1381	−30	2.1	1408	1410	2	0.1	(14) $\delta_{sym}(CH_3)$ 59, $\delta_{sym}(NH_3)$−25
1367(sh)		1383	1373	−10	0.7	1384	1346	−38	2.7	1387	1364	−23	1.7	(15) τ(HC$_\alpha$CO) 56, δ(HC$_\alpha$C$_\alpha$)13
1358(s)	1356(s)	1364	1328	−36	2.6	1363	1332	−31	2.3	1371	1169	−202	14.7	(16) $\nu_{sym}(CO_2)$, $\nu(C_\alpha$-C) -55
1304(m)	1305(m)	1313	1205	−108	**8.2**	1315	1250	−65	4.9	1310	1286	−24	1.8	(17) δ(HC$_\alpha$C$_\beta$) 47
1237(w)	1221(w)	1208	1403	195	**16.1**	1207	1328	121	**10.0**	1221	1188	−33	−2.7,	(18) τ(HNC$_\alpha$C$_\beta$) -27, τ(HC$_\beta$C$_\alpha$N) -23
1148(m)	1145(sh)	1126	1026	−100	**8.9**	1126	1101	-25	2.2	1132	1117	−15	1.3	(19) τ(HC$_\beta$C$_\alpha$N) 22, τ(HNC$_\alpha$C$_\beta$) 15
1112(m)	1114(m)	1102	1057	−45	4.1	1102	1040	−62	5.6	1122	1014	−108	**9.6**	(20) $\nu(C_\beta-C_\alpha)$ -28, τ(HNC$_\alpha$C$_\beta$) 20
1019(m)	1009(m)	1005	1170	165	**16.4**	1005	1158	153	**15.2**	1013	1019	6	0.6	(21) τ(HC$_\beta$C$_\alpha$N) 28, τ(HNC$_\alpha$C$_\beta$) -24
922(m)	924(m)	986	810	−176	**17.8**	987	977	−10	1.0	994	886	−108	**10.9**	(22) τ(HNC$_\beta$C$_\alpha$) -35, $\nu(C_\beta-C_\alpha)$ 28
851(s)	850(s)	885	862	−23	2.6	884	855	−29	3.2	914	915	1	0.1	(23) $\nu(C-C_\alpha)$ -61
		828	817	−11	1.3	827	818	−9	1.1	840	816	−24	2.9	(24) $\nu(C-C_\alpha)$ 44, $\delta(C_\alpha$CO) -19
771(m)	777(m)	770	825	55	7.1	768	797	29	3.8	770	764	−6	0.8	(25) w(OC$_\alpha$OC) -46, $\delta(C_\alpha$CO) -13
654(m)	630(w)	610	671	61	**10.0**	613	679	66	**10.8**	657	614	−43	6.5	(26) $\delta(C_\alpha$CO) 40, $\nu(C-C_\alpha)$ -17
533(m)	531(m)	516	557	41	7.9	517	521	4	0.8	528	507	−21	4.0	(27) $\delta(C_\alpha$CO) 56, $\nu(C-C_\alpha)$ -20
400(m)	410(w)	388	832	444	**114**	384	624	240	**62.5**	386	356	−30	7.8	(28) δ(C$_\beta$C$_\alpha$N) 63
321(w)	336(w)	332	320	−12	3.6	339	248	−91	**26.8**	337	448	111	**32.9**	(29) w(CC$_\beta$NC$_\alpha$) 51, δ(C$_\beta$C$_\alpha$N) 15
		269	179	−90	**33.5**	269	284	15	5.6	278	87	−191	**68.7**	(30) δ (C$_\alpha$CO) 68
		233	31	−202	**86.7**	236	7	−229	**97.0**	255	325	70	**27.5**	(31) τ(HC$_\beta$C$_\alpha$N) 85
		223	273	50	**22.4**	219	617	398	**182**	249	231	−18	7.2	(32) τ(HNC$_\alpha$C) 79
		57	184	127	**223**	56	459	403	**720**	53	118	65	**123**	(33) τ(NC$_\alpha$CO) 65, τ(HNC$_\alpha$C) -17

Designations: ν — valence stretching, δ — deformation scissor vibration (bending), τ — deformation torsional vibration (torsion), ω(ABCD) — a kind of torsional vibration, denotes the angle between AD vector and BCD plane, sym and asym — symmetric and asymmetric vibrations.

reference bands. The mid-intensity band at 1304 cm^{-1} (in the buffer — 1305 cm^{-1}) correlates with the angular vibration δ(HC$_\alpha$C$_\beta$).

Region below 1300 cm^{-1} The mid-intensity band at 1147 cm^{-1} and the low-intensity band at 1236 cm^{-1} correlate with deformation torsional vibrations τ(HNC$_\alpha$C$_\beta$) and τ(HC$_\beta$C$_\alpha$N). These bands in the buffer solution are quenched due to additional hydrogen bonds between the group $-NH_3$ and water molecules. The mid-intensive band at 1112 cm^{-1} (in the buffer 1114 cm^{-1}) is associated with antisymmetric stretching of couplings $\nu(C_\alpha-C_\beta H_3)$ and $\nu(C_\alpha-NH_3)$, which are mixed with torsional vibrations τ(HNC$_\alpha$C$_\beta$) and τ(HC$_\beta$C$_\alpha$N). The mid-intensity band at 1019 cm^{-1} corresponds to the deformation torsional vibrations τ(HNC$_\alpha$C$_\beta$) and τ(HC$_\beta$C$_\alpha$N). The mid-intensity band at 922 cm^{-1} (in the buffer — 924 cm^{-1}) correlates with deformation torsional vibrations τ(HNC$_\beta$C$_\alpha$) which is mixed with a stretching $\nu(C_\alpha-C_\beta)$. The most intense reference band of alanine at 851 cm^{-1} (in the buffer — 850 cm^{-1}) corresponds, according to calculations, to the symmetric stretching of couplings with Cα-atom: $\nu(C_\alpha-NH_3)$, $\nu(C\alpha^-CO_2)$ and $\nu(C_\alpha-CH_3)$. The mid-intensity band at 771 cm^{-1} (in the buffer — 777 cm^{-1}) corresponds to the deformation vibration ω(OC$_\alpha$OC) with the addition of angular bend δ(C$_\alpha$C$_\beta$N). The mid-intensity band at 652 cm^{-1} is associated with the deformation scissor vibration $\delta(C_\alpha$CO) and the stretching of $\nu(C-C_\alpha)$, this

Table 3. Experimental RS bands (cm^{-1}) of glycine and alanine in buffer solution and harmonic frequencies (cm^{-1}) of discrete-continuum models of Gly(ZW)+7H_2O and Ala(ZW)+7H_2O obtained by B3LYP+GD3

Buffer	Gly(ZW)+7H_2O (Scaled*)	Gly(ZW)+7H_2O	Number and type vibrations	Buffer	Ala(ZW)+7H_2O (Scaled**)	Ala(ZW)+7H_2O	Number and type vibrations
					3146	3344	(84) ν(O−H)
	3173	3343	(75)ν(O−H)		3090	3284	(83) ν(O−H), $\nu_{asym}(NH_2)$
3148 (sh)	3123	3290	(74) ν(O−H), $\nu_{asym}(NH_2)$	3070(sh)	3060	3252	(82) ν(N−H), $\nu_{sym}(NH_2)$
3078 (sh)	3077	3242	(73) $\nu_{asym}(NH_2)$	2998 (s)	2988	3176	(81) $\nu_{asym}(NH_2)$
	3026	3188	(72) $\nu_{sym}(NH_2)$		2955	3140	(80) ν(N−H), $\nu(C_\alpha{-}H)$
3014 (s)	3010	3171	(71)$\nu_{asym}(C_\alpha H_2)$	2950 (s)	2950	3135	(79) $\nu(C_\alpha{-}H)$, $\nu_{sym}(C_\alpha H_2)$
2973(s)	2973	3132	(70) ν(N−H)		2936	3120	(78) $\nu(C_\alpha{-}H)$ $-\nu_{asym}(C_\beta H_2)$
	2939	3096	(69) $\nu_{sym}(C_\alpha H_2)$	2925 (sh)	2930	3114	(77) $\nu(C_\alpha{-}H)$ $-\nu(C_\alpha{-}H)$
				2894 (s)	2867	3046	(76) $\nu_{sym}(C_\beta H_3)$
	1678	1709	(68) δ(HNH), $\delta(H_2O)$		1679	1710	(75) δ (HNH), $\nu_{as}(CO_2)$, $\delta(H_2O)$
	1673	1703	(67) δ(HNH), $\nu_{asym}(CO_2)$, $\delta(H_2O)$		1672	1703	(74) δ(HNH), $\nu_{as}(CO_2)$, $\delta(H_2O)$
	1653	1682	(66) δ(HNH), $\delta(H_2O)$		1643	1674	(73) δ(HNH), $\delta(H_2O)$
1626(w)	1644−1599	1673−1627	(65)-(60) $\delta(H_2O)$		1642	1673	(72) δ(HNH), $\delta(H_2O)$
	1565	1593	(59) $\delta_{sym}(NH_3)$, $\nu_{asym}(CO_2)$, $\delta(H_2O)$	1610(w)	1630−1599	1660−1628	(71)-(67) $\delta(H_2O)$
	1548	1576	(58) $\delta_{sym}(NH_3)$, $\nu_{asym}(CO_2)$, $\delta(H_2O)$		1561	1589	(66) $\delta_{sym}(NH_3)$, $\nu_{as}(CO_2)$, $\delta(H_2O)$
					1545	1574	(65) $\delta_{sym}(NH_3)$, $\nu_{as}(CO_2)$, $\delta(H_2O)$
				1464(s)	1467	1494	(64) $\delta(HC_\beta H)$, $\tau(HC_\beta C_\alpha N)$
1446(m)	1464	1489	(57) $\delta_{sym}(C_\alpha H_2)$		1459	1486	(63) $\delta(HC_\beta H)$, $\tau(HC_\beta C_\alpha N)$
1415(m)	1415	1440	(56) $\nu_{sym}(CO_2)$, $\nu(C_\alpha\text{-}C)$	1414(m)	1414	1440	(62) $\delta_{sym}(CH_2)$, $\nu(C_\alpha\text{-}C)$, $\tau(HC_\alpha CO)$
	1351	1375	(55) $\tau(HC_\alpha CO)$, $\nu_{sym}(CO_2)$	1380 (w)	1391	1416	(61) $\delta_{sym}(CH_3)$, $\tau(HC_\alpha CO)$
1330 (s)	1340	1363	(54) δ(HCN), $\tau(HC_\alpha CO)$, $\tau(HNC_\alpha C)$	1356(s)	1378	1403	(60) $\nu(C_\alpha{-}C)$, ν(O=C), $\delta_{sym}(CH_3)$
				1304 (m)	1325	1349	(59) $\delta(HC_\alpha C_\beta)$, ν(O=C)
	1200	1222	(53) $\tau(HNC_\alpha C)$, δ(HNH)	1221 (w)	1244	1267	(58) $\tau(HC_\beta C_\alpha N)$, $\tau(HNC_\alpha C_\beta)$
1128 (w)	1140	1160	(52) $\tau(HNC_\alpha C)$, δ(HNH)	1142 (sh)	1193	1215	(57) $\tau(HNC_\alpha C_\beta)$, $\tau(HC\beta C\alpha N)$
1034 (m)	1004	1022	(51) $\nu(C_\alpha{-}N)$	1114 (m)	1100	1120	(56) $\nu(C_\alpha{-}C_\beta)$, $\nu(C_\alpha\text{-}N)$
	946	962	(50) $\tau(HNC_\alpha C)$		1025	1044	(55) $\tau(HC_\beta C_\alpha N)$, $\tau(HNC_\alpha C_\beta)$
				1009 (m)	1008	1027	(54) $\tau(HC_\beta C_\alpha{-}N)$, $\nu(C_\alpha{-}C_\beta)$
				924 (m)	912	929	(53) $\nu(C_\alpha\text{-}N)$, $\nu(C_\alpha{-}C)$

Table 3 (*continued*)

Buffer	Gly(ZW)+7H_2O (Scaled*)	Gly(ZW)+7H_2O	Number and type vibrations	Buffer	Ala(ZW)+7H_2O (Scaled**)	Ala(ZW)+7H_2O	Number and type vibrations
899(s)	899	914	(49) $\nu(C_\alpha-C)$, $\delta(C_\alpha CO)$		881	898	(52) $\tau(HNC_\alpha C_\beta)$, $\tau(H_2O)$
				850 (s)	854	870	(51) $\nu(C_\alpha-N)$, $+\nu(C_\alpha-C)$, $\delta(CO_2)$
	877−769	893−783	(48)-(44) $\tau(H_2O)$		848	864	(50) $\tau(H_2O)$
	746	759	(43) $\tau(HC_\alpha CO)$, $\tau(H_2O)$		811	826	(49) $\nu(C_\alpha$-C), $\delta(CO_2)$, $\tau(H_2O)$
	726	738	(42) $\tau(HC_\alpha CO)$, $\tau(H_2O)$		802	816	(48) $\tau(HNC_\alpha C_\beta)$, $\tau(H_2O)$
	695−653	707−665	(40)−(41) $\tau(H_2O)$	778 (m)	783	799	(47) $\omega(C_\alpha OC)$, $\delta(C_\alpha CO)$
672(w)	621	632	(39) $\delta(C_\alpha CO)$, $\nu(C_\alpha-C_\beta)$, $\tau(H_2O)$		772−690	786−703	(46)−(44) $\tau(H_2O)$
585 (w)	598	609	(38) $\tau(HC_\alpha CO)$, $\tau(HNC_\alpha C)$	630 (w)	662	675	(43) $\delta(C_\alpha CO)$, $\nu(C_\alpha$-N), $\nu(C_\alpha$-C)
	573	583	(37)$\tau(H_2O)$, $\tau(HNC_\alpha C)$		657−556	670−566	(42)−(40) $\tau(H_2O)$, $\tau(HNC_\alpha C)$
	527	536	(36) $\tau(HNC_\alpha C)$, $\tau(H_2O)$	531 (m)	540	550	(39) $\delta(C_\alpha CO)$, $\nu(C_\alpha$-C)
	486	495	(35) $\tau(H_2O)$, $\tau(HNC_\alpha C)$		512	521	(38) $\tau(HNC_\alpha C)$, $\tau(H_2O)$
507 (m)	471	480	(34) $\delta(C_\alpha CO)$, $\nu(C_\alpha$-C), $\nu(C_\alpha-N)$		481	489	(37) $\tau(H_2O)$, $\tau(HNC_\alpha C)$
	467	476	(33) $\tau(HNC_\alpha C)$, $\tau(H_2O)$		451	460	(36) $\tau(HNC_\alpha C)$, $\tau(H_2O)$
	441	449	(32) $\tau(HC_\alpha CO)$, $\tau(H_2O)$		444	452	(35) $\tau(H_2O)$, $\tau(HNC_\alpha C)$
	427	435	(31) $\tau(H_2O)$		424	431	(34) $\tau(H_2O)$
	413	420	(30) $\tau(HC_\alpha CO)$,$\tau(H_2O)$		413	420	(33) $\tau(H_2O$
	405	412	(29) $\tau(H_2O)$, $\tau(HNC_\alpha C)$		393	400	(32) $\tau(H_2O)$
320(w)	326	331	(28) $\delta(CC_\alpha N)$	410 (w)	383	390	(31) $\delta(NC_\alpha C_\beta)$, $\tau(H_2O)$
	289	295	(27) $\tau(HC_\alpha CO)$, $\tau(H_2O)$	336 (w)	327	333	(30) $\omega(CC_\beta NC_\alpha)$, $\tau(H_2O)$

* For glycine frequencies above 3000 cm^{-1} the magnification multiplier (MM) equal to 0.9492 was used, and in the region below 2000 cm^{-1} — MM = 0.9826.

(**) For alanine frequencies in the region above 3000 cm^{-1} the magnification multiplier 0.941 was used, and in the region below 2000 cm^{-1} — MM= 0.982.

band is severely blurred in the buffer due to additional torsional vibrations of water molecules associated with the $-CO_2$ group. The band of average intensity at 533 cm^{-1} (in the buffer — 531 cm^{-1}) corresponds to deformation scissor vibrations of the skeleton structure $\delta(NC_\alpha C_\beta)$ and $\delta(C_\alpha CO)$, to which the stretching of $\nu(C_\alpha-CO_2$ is mixed). he bands of low intensity at 400 cm^{-1} (in the buffer — 410 cm^{-1}) and 321 cm^{-1} (in the buffer — 336 cm^{-1}) correlate with the deformation vibration $\omega(CC_\beta NC_\alpha)$ and torsional vibrations of group -NH_3. These bands are strongly blurred in the buffer solution due to the collective torsional vibrations of water molecules associated with the amino group.

Visual comparison of experimental and calculated RS spectra for discrete-continuum models Gly(ZW)+7H_2O and Ala(ZW)+7H_2O are shown in Fig. 3. The numbering of vibrational modes corresponds to the data from Table 3. For glycine frequencies in the region above 3000 cm^{-1}, a magnification multiplier of 0.9492 was used, and in the region below 2000 cm^{-1} — a multiplier of 0.9826. The alanine frequencies were scaled by multipliers 0.941 in the region above 3000 cm^{-1} and 0.982 in the region below 2000 cm^{-1}. It can be seen that the harmonic approximation provides a good agreement of the main characteristic bands of RS spectra of glycine and alanine in the region of 300−1800 cm^{-1}.

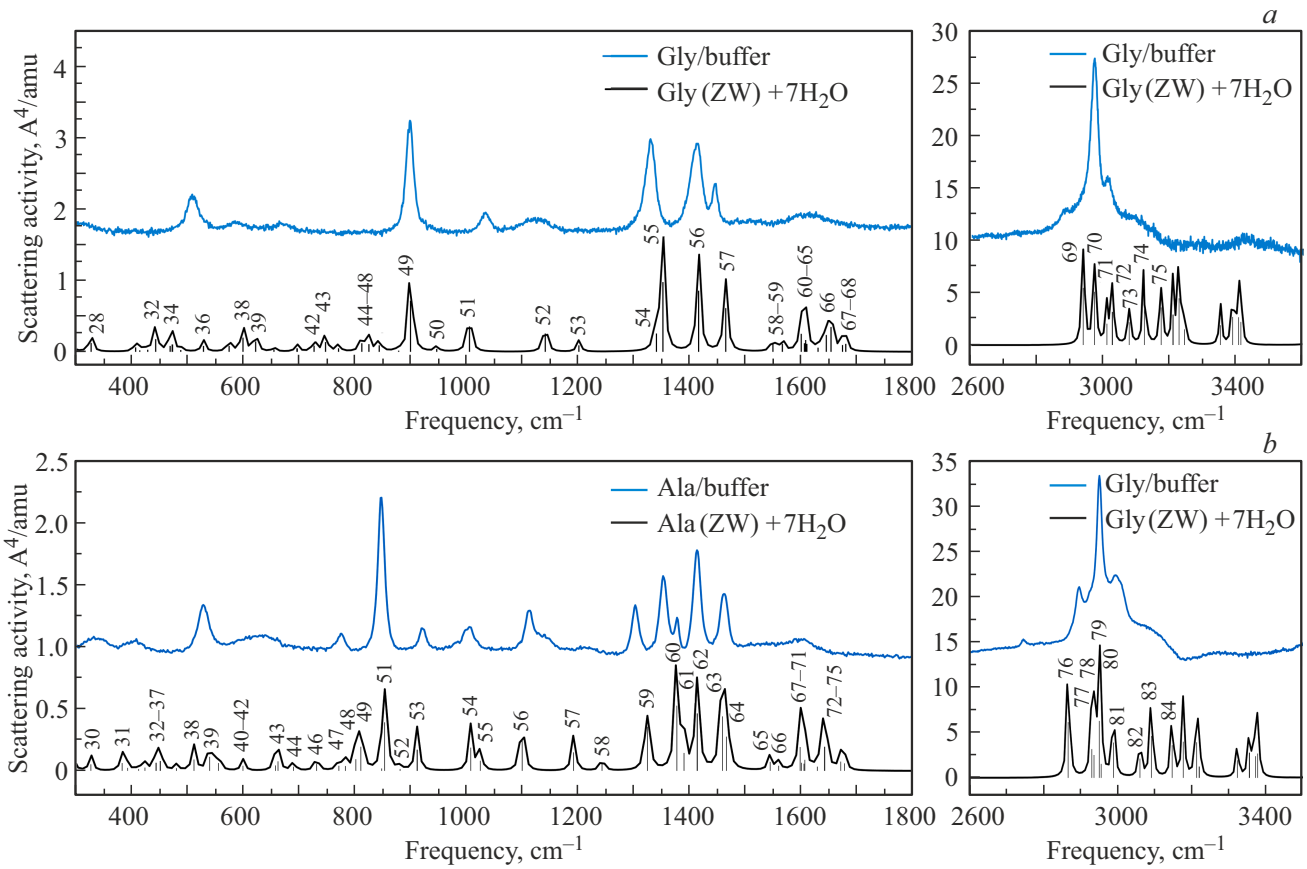

Figure 3. Experimental RS spectra of glycine (a) and alanine (b) in the buffer solution and designed RS spectra for models Gly(ZW)+7H_2O and Ala(ZW)+7H_2O.

Anharmonic calculations of Gly(ZW) and Ala(ZW) zwitterions

Taking into account Fermi and Darling-Dennison resonances is important for obtaining accurate vibrational frequencies and intensities, as well as for the correct interpretation of experimental spectra. The Fermi resonance occurs when the fundamental vibrational mode has a frequency close to the overtone frequency or combination frequency: $\omega_1 \approx \omega_2 + \omega_3$. The key step of anharmonic calculations in this case is the calculation of cubic anharmonic constants k_{ijk}. These constants describe how the energy of the system changes when three normal modes are excited simultaneously. Cubic anharmonic constants are the third derivatives of energy with respect to normal coordinates at the equilibrium point: $k_{ijk} = (\partial^3 V/\partial q_i \partial q_j q_k)|r = r_e$ are found in Gaussian 16 by method of numerical differentiating. Unlike Fermi resonances, which are the result of cubic interaction, Darling-Dennison resonances are associated with the interaction of four vibrational modes. They arise when there are two vibrational states that satisfy certain conditions in terms of energy and symmetry and interact through quartic terms in the expansion of potential energy: $k_{ijk} = (\partial^4 V/\partial q_i \partial q_j \partial q_k)|r = r_e$. In the simplest case, Darling-Dennison resonance $(2-2)$ occurs between two overtones or two combination frequencies that have similar energies: $\omega_1 + \omega_2 \approx \omega_3 + \omega_4$. Also Gaussian 16 may account for Darling-Dennison resonances (1-1) and (1-3): $\omega_1 \approx \omega_2$ and $\omega_1 \approx \omega_2 + \omega_3 + \omega_4$. Although Darling-Dennison resonances are usually weaker than Fermi resonances, they can have a significant effect on vibrational spectra, especially in molecules with high symmetry.

The presence of numerous stretchings in amino acids like ν(C −H), ν(N−H) and ν(C=O), as well as deformation angular bends like δ(H−C−H), δ(H−N−H) and δ(O=C=O) indicates that a strong interaction may exist between them. To clarify the values of the vibrational modes, we made an anharmonic analysis of Gly(ZW) and Ala(ZW) zwitterions using GVPT2 method, taking into account Fermi (1-2) and Darling-Dennison resonances (1-1) and (2-2) at the level of functional density B3LYP(+GD3)/def2TZVPP and perturbation theory MP2(FC)/def2TZVPP. Theoretically, it was expected that the values of anharmonic frequencies would be shifted to the low frequency range relative to the harmonic frequencies. The measure of frequency shift can be both absolute $\Delta\nu = \nu^{\text{harm}} - \nu^{\text{anh}}$ and relative $-\Delta\nu| \cdot 100\%/\nu^{\text{harm}}$ (as a percentage of the harmonic frequency) anharmonic shifts. Typically, an anharmonic shift is considered strong if the percentage change in frequency exceeds the threshold of 5%, and very strong if

Table 4. Harmonic and anharmonic frequencies (cm^{-1}) of Gly(ZW) zwitterion, their absolute ($\Delta\nu = \nu^{harm} - \nu^{anh}$) and relative $\left(\frac{|\Delta\nu|}{harm} \cdot 100\%\right)$ shifts obtained by B3LYP/def2TZVPP method when some vibrational modes are„deactivated"

Experiment		SkipPT2=Modes 1				SkipPT2=Modes 1, 2			SkipPT2=Modes 1,2,3			Number and type of vibrations
crystal	buffer ν^{harm}	ν^{anh}	$\Delta\nu$	$\frac{\lvert\Delta\nu\rvert}{\nu^{harm}}$	ν^{anh}	$\Delta\nu$	$\frac{\lvert\Delta\nu\rvert}{\nu^{harm}}$	ν^{anh}	$\Delta\nu$	$\frac{\lvert\Delta\nu\rvert}{\nu^{harm}}$		
3145 (m)	3148(sh)	3552	3365	−187	5.3	3353	−199	5.6	3352	−200	5.6	(24) $\nu_{asym}(NH_2)$
	3078 (sh)	3498	3328	−170	4.9	3322	−175	5.0	3321	−176	5.0	(23) $\nu_{sym}(NH_2)$
3007 (s)	3014(s)	3171	3011	−160	5.0	3013	−158	5.0	3014	−157	5.0	(22) $\nu_{asym}(C_\alpha H_2)$
		3146	2774	−372	**11.8**	2756	−390	**12.4**	2837	−310	**9.9**	(21) ν(V−H)
2973 (s)	2973 (s)	3113	2994	−119	3.8	2985	−128	4.1	2988	−126	4.0	(20) $\nu_{sym}(C_\alpha H_2)$
1670 (w)		1664	1625	−39	2.3	1633	−31	1.9	1636	−28	1.7	(19) δ(HNH), ν_{asym} (CO_2)
1630 (w)	1626 (w)	1656	1636	−20	1.2	1598	−58	3.5	1601	−54	3.3	(18) δ(HNH)
1570 (w)		1640	1478	−162	**9.9**	1527	−112	6.8	1520	−120	7.3	(17) δ(HNH), ν_{asym} (CO_2)
1455 (m)		1475	1440	−35	2.4	1448	−27	1.8	1452	−23	1.6	(16) $\tau(HC_\alpha CO)$, δ_{sym} ($HC_\alpha H$)
1440 (m)	1446(m)	1446	1377	−70	4.8	1365	−81	5.6	1376	−71	4.9	(15) $\delta_{sym}(NH_3)$, $\delta_{sym}(HC_\alpha H)$
1413 (m)	1415 (m)	1373	1322	−51	3.7	1318	−55	4.0	1323	−50	3.6	(14) $\nu_{sym}(CO_2)$, $\nu(C_\alpha-C)$
1325 (s)	1330 (s)	1332	1265	−67	5.0	1269	−63	4.7	1273	−59	4.4	(13) $\delta_{sym}(HC_\alpha H)$, $\tau(HC_\alpha CO)$
		1309	1259	−50	3.8	1264	−45	3.4	1266	−43	3.3	(12) δ(HCN)
1140 (w)	1128 (w)	1112	81	−131	**11.8**	1004	−108	**9.7**	1008	−104	**9.4**	(11) $\tau(HNC_\alpha C)$, δ(HNH)
1108 (w)		1103	1046	−57	5.2	1045	−58	5.3	1053	−50	4.5	(10) $\tau(HNC_\alpha C)$, δ(HNH)
1034 (m)	1034 (m)	993	924	−69	6.9	930	−63	6.3	931	−62	6.2	(9) $\nu(N-C_\alpha)$
925 (w)		940	849	−91	**9.8**	875	−66	7.0	879	−62	6.6	(8) $\tau(HNC\alpha C)$, δ(HCN)
892 (s)	898 (s)	867	848	−19	2.2	846	−21	2.4	847	−20	2.3	(7) $\nu(C\alpha-C)$, $\delta(C_\alpha CO)$
700 (w)	672 (w)	676	666	−10	1.5	670	−6	0.9	666	−10	1.5	(6) $\delta(C_\alpha CO)$, $\nu(C_\alpha-C)$
603 (m)	585 (w)	577	577	0	0	586	9	1.6	587	10	1.7	(5) $\tau(HC_\alpha CO)$, $\tau(HNC_\alpha C)$
486 (w)	507 (w)	500	493	−7	1.4	496	−4	0.8	494	−6	1.2	(4) $\delta(C_\alpha CO)$, $\nu(C_\alpha-C)$
360 (w)		298	230	−68	**22.8**	249	−49	**16.4**	298	0	0	(3) $\delta(C_\alpha CO)$
		269	131	−139	**51.7**	271	2	0.7	271	2	0.7	(2) τ ($HNC_\alpha C$)
		110	113	3	2.7	113	3	2.7	113	3	2.7	(1) $\tau(HNC_\alpha C)$, $\tau(HC_\alpha CO)$

the threshold is above 10%. It turned out that calculations using B3LYP(+GD3) and MP2(FC) methods give both positive and unreasonably large negative anharmonic shifts for some fundamental frequencies (Table 1, 2). The strongest anharmonic shifts are highlighted in Tables 1, 2 in bold.

It can be seen that in the frequency range above $3000\,cm^{-1}$ strong ($\sim 5\%$) anharmonic shifts prevail for many valence bond extensions ν(With−H) and ν(N−H), which is in better agreement with experiment compared to harmonic frequencies. However, for some oscillatory modes, unreasonably strong anharmonic corrections ($> 10\%$) are observed, and they differ for the selected calculation methods. So, for Ala(ZW) zwitterion B3LYP+GD3 method provides a strong shift for the vibrational mode (31) of ν(N−H) kind, B3LYP method (neglecting the dispersion) — for the vibrational mode (30) of $\nu(C_\beta-H)$, and MP2(FC) method — for a mixed mode (28) like $\nu(C_\alpha-H)$-$\nu(C_\beta-H)$. A similar situation occurs for the vibrational modes (20) and (21) of Gly(ZW). This is explained by the difference in the found vibrational mode energies for the calculation methods, which in turn leads to their inclusion or omission in the Fermi and Darling-Dennison resonances.

In the frequency range $1500-1700\,cm^{-1}$ moderate anharmonic shifts of deformational angular bends δ(HNH) are observed. However, for the vibrational mode of glycine (17) and vibrational mode of alanine (24) , the calculations yielded very strong negative shifts. This is due to both Fermi resonances arising between the valence stretching of ν(N−H) coupling and the overtones of deformational angular bends δ(HNH) and Darling-Dennison resonances (1−1) between the angular fluctuations (17) and (19) of Gly(ZW) zwitterion and the angular fluctuations (24) and (26) of Ala(ZW). It can also be noted that B3LYP+GD3 method gives strong positive shifts for frequencies in this region, which is inconsistent with experimental data.

In the frequency range $1200-1500\,cm^{-1}$ anharmonic analysis of Gly(ZW) and Ala(ZW) zwitterions gives a rather contradictory pattern due to frequency mixing and ambiguous results obtained by various methods. Nevertheless, comparable shifts for most frequencies were obtained using B3LYP and MP2 methods. According to B3LYP, the Gly(ZW) zwitterion has a strong Fermi resonance between the main vibrational mode (14) and a combination of vibrations (7)+(4), as well as moderate Darling-Dennison resonances (1-1) between vibrational modes (14) and (13), (15) and (14), (16) and (15). Analysis of Ala(ZW) zwitterion

Table 5. Harmonic and anharmonic frequencies (cm^{-1}) of Ala(ZW) zwitterion, their absolute ($\Delta\nu = \nu^{harm} - \nu^{anh}$) and relative $\left(\frac{|\Delta\nu|}{\nu^{harm}} \cdot 100\%\right)$ shifts obtained by B3LYP/def2TZVPP method when some vibrational modes are„deactivated“

Experiment		SkipPT2=Modes 1				SkipPT2= =Modes 1,2			SkipPT2= =Modes 1,2,3			SkipPT2= =Modes 1,2,3,6			Number and type of vibrations
Crystal	Buffer	ν^{harm}	ν^{anh}	$\delta\nu$	$\frac{\lvert\Delta\nu\rvert}{\nu^{harm}}$	ν^{anh}	$\Delta\nu$	$\frac{\lvert\Delta\nu\rvert}{\nu^{harm}}$	ν^{anh}	$\Delta\nu$	$\frac{\lvert\Delta\nu\rvert}{\nu^{harm}}$	ν^{anh}	$\Delta\nu$	$\frac{\lvert\Delta\nu\rvert}{\nu^{harm}}$	
3083 (m)	3070 (sh)	3545	3363	−182	5.1	3359	−186	5.2	3355	−190	5.4	3354	−191	5.4	(33) ν_{asym} (NH_2)
		3487	3312	−175	5.0	3303	−184	5.3	3313	−173	5.0	3311	−175	5.0	(32) $\nu_{sym}(NH_2)$
3000 (s)	2998 (s)	3139	3000	−139	4.4	3036	−103	3.3	2992	−147	4.7	3001	−138	4.4	(31) ν(N−H)
2985 (s)		3136	2737	−400	**12.8**	2698	−439	**14.0**	2779	−357	**11.4**	2775	−361	**11.5**	(30)ν(C_β-H)
2965 (s)	2950 (s)	3109	3021	−87	2.8	2997	−112	3.6	3011	−98	3.2	2991	−118	3.8	(29) ν(C_α-H)-ν_{asym}($C_\beta H_2$)
2933 (s)	2925 (sh)	3092	2967	−125	4.0	2970	−121	3.9	2959	−133	4.3	2958	−134	4.3	(28) ν(C_α−H) - ν(C_β−H)
2891 (m)	2894 (s)	3041	2894	−147	4.8	2960	−81	2.7	2962	−79	2.6	2951	−90	3.0	(27) $\nu_{sym}(C_\beta H_3)$
1633 (w)	1610 (w)	1659	1574	−86	5.2	1747	88	5.3	1686	30	1.8	1670	11	0.7	(26) δ(HNH), τ($HNC_\alpha C_\beta$)
1596 (m)		1649	1618	−31	1.9	1617	−32	1.9	1621	−28	1.7	1620	−29	1.8	(25) $\nu_{as}(CO_2)$, δ(HNH)
1550 (w)		1623	1781	159	**9.8**	1570	−53	3.3	1577	−46	2.8	1576	−47	2.9	(24) δ(HNH), $\nu_{as}(CO_2)$
1482 (m)		1488	1518	29	1.9	1486	−2.0	0.1	1485	−3.0	0.2	1464	−24	1.6	(23) δ(HCH), τ($HC_\beta C_\alpha$N)
1462 (s)	1464 (s)	1484	1472	−12	0.8	1456	−28	1.9	1451	−34	2.3	1449	−35	2.4	(22) δ(HCH), τ($HC_\beta C_\alpha$N)
1408 (m)	1414(m)	1434	1437	3.0	0.2	1439	5.0	0.3	1432	−2.0	0.1	1434	0	0	(21) $\delta_{sym}(NH_3)$, $\delta_{sym}(CH_3)$
1378 (sh)	1380 (w)	1411	1365	−46	3.3	1369	−42	3.0	1371	−40	2.8	1372	−39	2.8	(20) $\delta_{sym}(CH_3)$, $\delta_{sym}(NH_3)$
1367 (sh)		1384	1326	−58	4.2	1324	−60	4.3	1341	−43	3.1	1339	−45	3.3	(19)τ(HC_αCO), δ($HC_\alpha C_\beta$)
1358 (s)	1356 (s)	1363	1346	−17	1.2	1337	−26	1.9	1322	−41	3.0	1326	−37	2.7	(18) $\nu_{sym}(CO_2)$, ν(C_α−C)
1304 (m)	1305 (m)	1315	1273	−43	3.3	1274	−41	3.1	1272	−43	3.3	1273	−42	3.2	(17) δ($HC_\alpha C_\beta$)
1237 (w)	1221(w)	1207	1313	106	**8.8**	1271	64	5.2	1261	54	4.5	1238	31	2.6	(16) τ($HNC_\alpha C_\beta$), τ($HC_\beta C_\alpha$N)
1148 (m)	1145 (sh)	1126	1096	−30	2.7	1128	2.0	0.2	1114	−12	1.1	1112	−14	1.2	(15) τ($HC_\beta C_\alpha$N), τ ($HNC_\alpha C_\beta$)
1112 (m)	1114 (m)	1102	1132	30	2.7	1089	−13	1.2	1076	−27	2.5	1076	−26	2.4	(14) ν(C_β-C_α), τ ($HNC_\alpha C_\beta$)
1019 (m)	1009 (m)	1005	1051	46	4.6	1046	41	4.1	1029	25	2.5	1027	23	2.3	(13) τ($HC\beta C_\alpha$N), τ($HNC_\alpha C_\beta$)
922 (m)	924 (m)	987	988	1.0	0.1	981	−6.0	0.6	979	−8.0	0.8	983	−4.0	0.4	(12) τ($HNC_\alpha C_\beta$), ν(C_β−C_α)
851 (s)	850 (s)	884	852	−32	3.6	851	−33	3.7	853	−31	3.5	854	−30	3.4	(11) ν(C-C_α)
		827	820	−7.0	0.8	813	−14	1.7	814	−13	1.6	812	−15	1.8	(10) ν(C-C_α), δ(C_αCO)
771 (m)	777 (m)	768	785	17	2.2	778	10	1.3	775	7.0	0.9	772	3.0	0.4	(9) ω(OC_αOC), δ(C_αCO)
652 (m)	630 (w)	613	610	−3.0	0.5	609	−4.0	0.7	609	−4.0	0.7	609	−4.0	0.7	(8) δ(C_αCO), ν(C-C_α)
533 (m)	531 (m)	517	527	10	1.9	518	1.0	0.2	520	3.0	0.6	514	−3.0	0.6	(7) δ(C_αCO), ν(C-C_α)
400 (m)	410 (w)	384	639	255	**66.4**	545	161	**41.9**	548	164	**42.7**	384	0.0	0.0	(6) δ($C_\beta C_\alpha$N)
321 (w)	336 (w)	339	322	−17	5.0	315	−23	6.8	329	−10	2.9	342	3.0	0.9	(5) ω($CC_\beta NC_\alpha$), δ($C_\beta C_\alpha$N)
		269	240	−29	**10.8**	246	−23	**8.6**	251	−18	6.7	254	−15	5.6	(4) δ(C_αCO)
		236	359	123	**52.1**	435	199	**84.3**	237	1.0	0.4	237	1.0	0.4	(3) τ($HC_\beta C_\alpha$N)
		219	772	553	**253**	220	1.0	0.5	220	1.0	0.5	220	1.0	0.5	(2) τ($HC_\beta C_\alpha$N)
		56	58	2.0	3.6	58	2.0	3.6	58	2.0	3.6	58	2.0	3.6	(1) τ(NC_αCO), τ(HNC_αC)

found using B3LYP method showed that moderate Fermi resonances occur between the following vibrational modes: (22) ≈ (14) + (6), (19) ≈ (13) + (6) and (19) ≈ (9) + (8). Besides, noticeable Darling-Dennison resonances (1-1) are observed between the oscillatory frequencies (23) and (22), (23) and (21), (23) and (20), (22) and (20), (20) and (17), (19) and (18), (19) and (17).

In the frequency range below 1200 cm^{-1}, significant negative shifts were found for many anharmonic frequencies of Gly(ZW) and Ala(ZW) zwitterions. A particularly dramatic situation was observed for the lowest frequency torsion oscillations, the shifts of which turned out to be incredibly large. It is known that such shifts in anharmonic calculations occur due to the instability of numerical differentiation when calculating anharmonic constants, therefore, one of the calculated parameters is the differentiation step. We analyzed the anharmonic frequencies with both the standard STEP=0.025 and the recommended [18] STEP=0.01, yet we couldn't get the improved results for the low-frequency modes. This indicated the need to rule them out or „deactivate“ them during anharmonic analysis. The developers of GVPT2 method in Gaussian 16 have provided for such an option. Using the key RedDim=Inactive= *n* the modes can be excluded from consideration, thereby reducing the dimension of the vibrational problem. The key DataMod=SkipPT2=Modes is a softer solution that allows for the modes to be included in the analysis, however, VPT2 procedure is not envisaged for them here. In general, it is

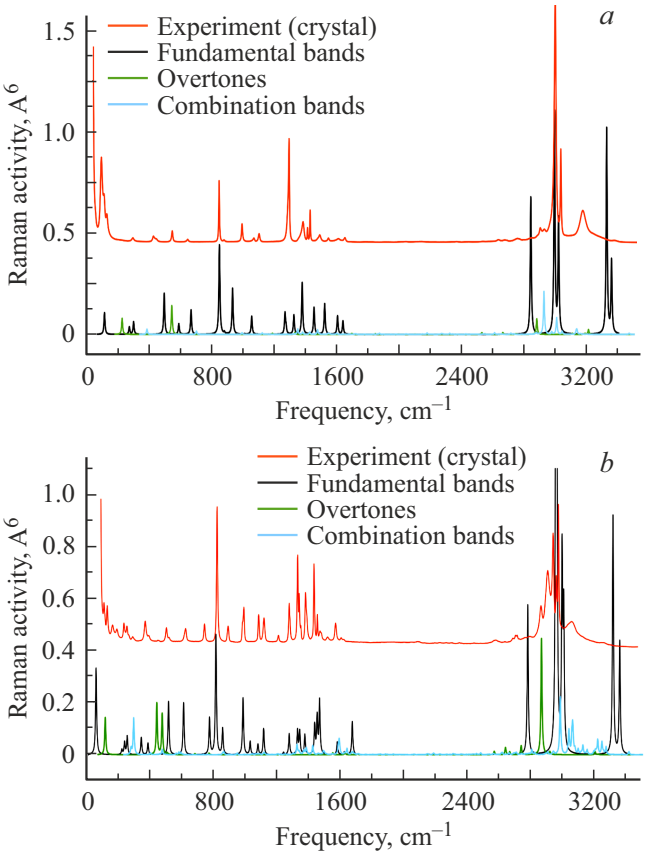

Figure 4. Experimental RS spectra of glycine (*a*) and alanine (*b*) in crystalline form and modelled anharmonic RS spectra for Gly(ZW) and Ala(ZW) modles.

recommended to use it to improve convergence and correct the non-physical results. In this regard, we made some additional anharmonic analysis at B3LYP/def2TZVPP level for Gly(ZW) and Ala(ZW) zwitterions removing one by one some low-frequency modes from the VPT2-procedure. The results of these calculations are listed in Tables 4, 5. Thanks to this, we were able to achieve acceptable agreement with the experimental data; at the same time, the low-frequency modes (1), (2) and (3) had to be deactivated for Gly(ZW) zwitterion, and for Ala(ZW) — low frequency modes (1), (2), (3) and (6) were removed. Next, the anharmonic RS spectra of Gly(ZW) and Ala(ZW) zwitterions were visualized allowing for the overtones and combination bands and correlated with the experimental spectra at reference frequencies of 892,cm^{-1} glycine and 851,cm^{-1} alanine (Fig. 4).

Conclusion

Using B3LYP+GD3/def2TZVPP method in the harmonic analysis the discrete-continuum models of Gly(ZW)+7H_2O and Ala(ZW)+7H_2O zwitterions were verified. It is shown that the experimental RS spectra of glycine and alanine in buffer solution are well reproduced by simply scaling the fundamental harmonic frequencies for these models of zwitterions.

As shown by the anharmonic analysis of Gly(ZW) and Ala(ZW) zwitterions using GVPT2 method, the allowance for Fermi and Darling-Dennison resonances does not automatically lead to a better agreement with the experiment. Only in the frequency range above 3000 cm^{-1} the anharmonic corrections significantly improve agreement with experimental data. In the frequency range 1200–1500 cm^{-1}, we were unable to uniquely identify all experimental bands due to the mixing of anharmonic frequencies and the ambiguity of the results obtained by various methods. In the frequency range below 1200 cm^{-1}, very strong, improbable shifts were obtained for the lowest frequency torsional vibrations. Yet, based on the density functional theory B3LYP/def2TZVPP (neglecting the dispersion) and perturbation theory MP2(FC)/def2TZVPP the comparable anharmonic shifts were obtained for many fundamental frequencies of Gly(ZW) and Ala(ZW) zwitterions. This indicates the need for such comparative calculations to eliminate the errors in interpretation. It should be noted that GVPT2 method provides acceptable agreement with experimental spectra if some low-frequency modes are disabled during VPT2 analysis. However, such a procedure shall be carried out carefully, consistently correcting the non-physical results. Despite the above, allowing for the anharmonic effects is a milestone on the way to a more accurate interpretation of vibrational spectra, although it requires much effort even for relatively small molecules.

Acknowledgments

The team of authors expresses its gratitude to Vladimir N. Bocharov, an employee of the Resource Center „Geomodel" Faculty of Physics of St. Petersburg State University, for advice and assistance in obtaining experimental spectra. We also express our gratitude to the staff of the High-Performance Center of St. Petersburg State University for their technical support in providing computational resources and software.

Conflict of interest

The authors declare that they have no conflict of interest.

References

[1] A.G. Csaszar, A. Perczel. Progress in Biophysics & Molecular Biology, **71**, 243 (1999).
[2] F.R. Tortonda, J.-L. Pascual-Ahuir, E. Silla et al. J. Chem. Phys., **109** (2), 592 (1998). DOI: 10.1063/1.476596
[3] B.Z. Chowdhry, T.J. Dines, S. Jabeen, R. Withnall. J. Phys. Chem. A, **112** (41), 10333 (2008). DOI: 10.1021/jp8037945
[4] A. Barth. Progress in Biophysics & Molecular Biology, **74**, 141 (2000). DOI: 10.1016/ s0079-6107(00)00021-3
[5] *Optical Spectroscopy and Computational Methods in Biology and Medicine* (Ed. by M. Baranska, Springer, 2014). DOI 10.1007/978-94-007-7832-0

[6] N. Derbel, B. Hernandez, F. Pfluger et al. Phys. Chem. B, **111**, 1470 (2007). DOI: 10.1021/jp0633953
[7] B. Hernandez, F. Pfluger, M. Nsangou, M. Ghomi. J. Phys. Chem. B, **113**, 3169 (2009). DOI: 10.1021/jp809204d
[8] N. Vyas, A.K. Ojha, A. Maternyb. Vibrational Spectroscopy, **55**, 69 (2011). DOI: 10.1016/ j.vibspec.2010.08.007
[9] I.V. Krauklis, A.V. Tulub, A.V. Golovin, V.P. Chelibanov. Opt. Spectrosc., **128** (10), 1598 (2020). DOI: 10.1134/S0030400X20100161
[10] S. Xu, J.M. Nilles, K.H. Bowen. J. Chem. Phys., **119** (20), 10696 (2003). DOI: 10.1063/ 1.1620501
[11] S.M. Bachrach. J. Phys. Chem. A, **112**, 3722 (2008). DOI: 10.1021/jp711048c
[12] J.-Y. Kim, D.-S. Ahn, S.-W. Park, S. Lee. RSC Adv., **4**, 16352 (2014). DOI: 10.1039/ C4RA01217H
[13] Alekseeva V.A., Krauklis I.V., Chizhov Y.V., Tulub A.V. J. Struct. Chem., **65**, 2272 (2024). DOI: 10.1134/S0022476624110143
[14] Gribov L.A. *Kolebaniya molekul* (Knizhniy dom „LIBRO-COM“, M., 2009). p. 544 (in Russian).
[15] P. Dančěk, J. Kapitán, V. Baumruk et al. J. Chem. Phys., **126**, 224513 (2007). DOI: 10.1063/1.2738065
[16] E. Fermi. Z. Phys., **71** (3–4), 250 (1931).
[17] B.T. Darling, D.M. Dennison. Phys. Rev., **57** (2), 128 (1940).
[18] V. Barone. J. Chem. Phys., **122**, 014108 (2005). DOI: 10.1063/1.1824881
[19] E.V. Boldyreva, T.N. Drebushchak, E.S. Shutova. Z. Kristallogr., **218**, 366 (2003). DOI: 10.1524/zkri.218.5.366.20729
[20] C. Tsuboi, K. Aburaya, F. Kimura et al. CrystEngComm., **18**, 2404 (2016). DOI: 10.1039/ C5CE02307F
[21] Resource Center „Geomodel“ SPbGU: https://researchpark.spbu.ru/index.php/geomodel-rus
[22] Magicplot Systems, LLC, 2021. https://magicplot.com/
[23] M.J. Frisch, G.W. Trucks, H.B. Schlegel et. al. Gaussian 16, Revision A.03, Gaussian, Inc., Wallingford CT, 2016.
[24] Computation Center of SPbGU: https://researchpark.spbu.ru/index.php/cc-rus
[25] M.H. Jamroz. Vibrational Energy Distribution Analysis: VEDA 4, program, Warsaw, 2004–2010. http://www.smmg.pl

Translated by T.Zorina